JACS
JOURNAL OF THE AMERICAN CHEMICAL SOCIETY

ARTICLE

pubs.acs.org/JACS

Structural Elucidation and Regioselective Functionalization of An Unexplored Carbide Cluster Metallofullerene $Sc_2C_2@C_s(6)$-C_{82}

Xing Lu,[†] Koji Nakajima,[†] Yuko Iiduka,[†] Hidefumi Nikawa,[†] Naomi Mizorogi,[†] Zdenek Slanina,[†] Takahiro Tsuchiya,[†] Shigeru Nagase,*[,‡] and Takeshi Akasaka*[,†]

[†]Life Science Center of Tsukuba Advanced Research Alliance, University of Tsukuba, Tsukuba, Ibaraki 305-8577, Japan

[‡]Department of Theoretical and Computational Molecular Science, Institute for Molecular Science, Okazaki, Aichi 444-8585, Japan

Supporting Information

ABSTRACT: A Sc_2C_{84} isomer, previously assumed to be $Sc_2@C_{84}$, is unambiguously identified as a new carbide cluster metallofullerene $Sc_2C_2@C_s(6)$-C_{82} using both NMR spectroscopy and X-ray crystallography. The ^{13}C-nuclei signal of the internal C_2-unit was observed at 244.4 ppm with a 15% ^{13}C-enriched sample. Temperature-dependent dynamic motion of the internal Sc_2C_2 cluster is also revealed with NMR spectrometry. Moreover, the chemical property of $Sc_2C_2@C_s(6)$-C_{82} is investigated for the first time using 3-triphenylmethyl-5-oxazolidinone (**1**) which provides a 1,3-dipolar reagent under heating. Regarding the low cage symmetry of this endohedral which contains 44 types of nonequivalent cage carbons, it is surprising to find that only one monoadduct isomer is formed in the reaction. Single-crystal X-ray results of the isolated pyrrolidino derivative $Sc_2C_2@C_s(6)$-$C_{82}N(CH_2)_2$Trt (**2**) reveal that the addition takes place at a [6,6]-bond junction, which is far from either of the two Sc atoms. Such a highly regioselective addition pattern can be reasonably interpreted by analyzing the frontier molecular orbitals of the endohedral. Electronic and electrochemical investigations reveal that adduct **2** has a larger highest occupied molecular orbital−lowest unoccupied molecular orbital (HOMO−LUMO) gap than pristine $Sc_2C_2@C_s(6)$-C_{82}; accordingly, it is more stable.

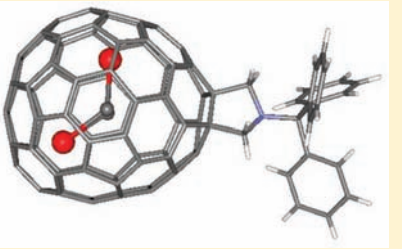

INTRODUCTION

The possibility of fullerenes to encapsulate metal atoms inside their hollow cages was predicted mere days after the discovery of the prototypical C_{60} and was verified by numerous subsequent results.[1] During the past two decades, various kinds of atoms and clusters have been entrapped inside fullerenes utilizing several synthetic methods, such as electric discharge, laser ablation, and ion implantation.[2] Among these new hybrid molecules generated so far, endohedral metallofullerenes (EMFs), i.e., fullerenes with metals or metallic clusters encapsulated inside, have attracted great attention because of the metal doping via electron transfer. As a result, EMFs have become a hot topic of research nowadays in materials science, physics, chemistry, and even biology with huge potential applications in electronics, photovoltaics, functional materials, and biomedicines.[3]

A wide variety of metallic species have been successfully encapsulated in fullerenes. In addition to conventional EMFs which contain purely metal atoms (usually one or two), such species encapsulating a cluster of metal carbide (M_2C_2/M_3C_2/M_4C_2), metal nitride (M_3N), metal oxide (M_2O/M_4O_2/M_4O_3), metal cyanide (M_3NC), or even metal sulfide (M_2S) are all successfully obtained, and most of them have been structurally characterized with single crystal X-ray diffraction (XRD) crystallography.[4−7] It is particularly interesting to find that among all the metals that can form EMFs macroscopically, only scandium gives rise to all the metallic species in EMFs observed so far. Accordingly, Sc-containing EMFs have received greater attention. Moreover, Sc-EMFs generally have higher production yields than EMFs containing other metals, which is another reason for their high attraction.[5]

However, the diversity and complexity of the internal metallic species hindered the complete exploration of many Sc-EMFs, although isolated macroscopically. In particular, scandium carbide EMFs are very interesting because two carbon atoms can be encapsulated together with several Sc atoms in the form of a carbide cluster, instead of participating in constructing the fullerene cage.[4] Consequently, structural identification of Sc-EMFs is very important and challenging. For example, the longstanding $Sc_3@C_{2v}(9)$-C_{82} proposed by the maximum entropy method coupled with Rietveld treatment of synchrotron powder diffraction data[4a] was recently revealed to be a carbide cluster metallofullerene, namely, $Sc_3C_2@I_h(7)$-C_{80} with both NMR and single crystal XRD methods.[4c] Moreover, the previously assigned $Sc_2@C_{82}$ and $Sc_2@C_{84}$ isomers have been recently determined to also be carbide EMFs, i.e., $Sc_2C_2@C_{2v}(5)$-C_{80} and $Sc_2C_2@C_{3v}(8)$-C_{82}, respectively.[4d,g] Obviously, structural elucidation of Sc-EMFs is a very meaningful and urgent work in fullerene research.

Meanwhile, the chemistry of EMFs has blossomed greatly as a result of the achievements in high-efficiency synthesis and isolation of some EMF species.[8] Furthermore, two main reasons

Received: September 20, 2011
Published: October 25, 2011

underscore the importance of chemical modifications of EMFs: (i) Functionalized EMFs bear more interesting properties than pristine EMFs and thus are more useful; (ii) EMF derivatives have a better chance of growing single crystals suitable for XRD measurement, which is regarded as the most reliable solution for EMF structures. During the past decade, great attention has been paid to the chemical properties of conventional EMFs and metal nitride cluster EMFs, for example M@C_{2v}(9)-C_{82} and M_3N@I_h-(7)-C_{80}, mainly because of their easy accessibility. Some unexpected behaviors of these EMFs, which differ completely from those of empty fullerenes because of the influence of the internal metals, are observed.[8] For example, strong interaction between the metal and the adjacent hexagonal carbon ring in La@C_{2v}(9)-C_{82} makes the part close to the metal highly reactive with electrophiles like carbene, while some cage carbons far from the encapsulated metal bear positive charges and therefore are more reactive toward nucleophiles, such as carbanions and dienes.[9] For metal nitride cluster EMFs, the cluster size is found critical to the chemical reactivity of the entire molecule. Numerous results related to the size-effect of nitride clusters on the chemical properties of EMFs have been reported. One interesting example reported by Echegoyen and co-workers showed that Sc_3N@C_{80} is obviously less reactive than Y_3N@C_{80} in both Prato and Bingel−Hirsch reactions due to the smaller cluster size of Sc_3N.[10] Thus, it appears conclusive that the internal metals exert fundamental influences on the properties, especially chemical reactivity, of EMFs.[8] However, in spite of recent achievements in the chemistry of conventional and nitride cluster EMFs, little is known about the chemical properties of other EMFs with a different metal core. While no report describes the chemical modifications of metal oxide, sulfide, and cyanide cluster EMFs, concern on the chemistry of metal carbide species is also very mute. The sole reaction performed on carbide EMFs is the cycloaddition of adamantylidene carbene, and only the structures of the corresponding derivatives were reported but no details about the reaction process and the chemical properties of the EMFs have been described in the relevant literatures.[4] A recent report on the Prato reaction of Sc_3C_2@C_{80} lacks X-ray structural data.[4i]

In this article, we first report the structural elucidation of a new carbide EMF, namely Sc_2C_2@C_s(6)-C_{82}, which was assumed as Sc_2@C_{84} in a previous study with NMR spectrometry and theoretical calculation.[11] Then we report for the first time the regioselective 1,3-dipolar addition reaction of this EMF with 3-triphenylmethyl-5-oxazolidinone (**1**) and the complete characterizations of the isolated monoadduct (**2**) including single-crystal XRD results and electrochemical studies.

EXPERIMENTAL SECTION

Materials and General Instruments. All reagents are commercially available, except the EMFs, which are synthesized with an improved direct current arc-discharge method, as reported before.[4c−g]

High- performance liquid chromatography (HPLC) was conducted on a LC-908 machine (Japan Analytical Industry Co., Ltd.) with toluene as mobile phase. Matrix-assisted laser desorption/ionization time-of-flight (MALDI-TOF) mass spectrometry was measured on a BIFLEX III spectrometer (Bruker, Germany) using 1,1,4,4-tetraphenyl-1,3-butadiene as a matrix. UV−vis NIR spectra were measured on a UV 3150 spectrometer (Shimadzu, Japan) in CS_2. Cyclic voltammogram (CV) and differential pulse voltammogram (DPV) were measured in 1,2-dichlorobenzene (ODCB) with 0.1 M of $(n\text{-}Bu)_4NPF_6$ at Pt working electrode with a potentiostat/galvanostat workstation (BAS CW-50). The scan rate of CV was 20 mV s^{-1}. Conditions of DPV: pulse amplitude, 50 mV; scan rate, 20 mV s^{-1}. The ^{13}C NMR spectra were measured on a Bruker AVANCE 500 spectrometer with a CryoProbe system in carbon disulfide using acetone-d_6 as an external lock. The ^{45}Sc NMR spectrum was measured in ODCB-d_4 at 146.0 MHz on a Bruker AVANCE 600 spectrometer. The ^{45}Sc chemical shift was calibrated with 1 M of Sc_2O_3/HCl (D_2O) as an external reference (0 ppm). XRD measurement was performed on a Bruker APEX II machine equipped with a CCD camera. The structure was solved with a direct method and was refined using SHLEX 97.[12]

Theoretical calculations were carried out using the Gaussian 03 program package.[13] The molecular structures were optimized at the B3LYP/3-21G(d)[14] with the B3LYP density functional.[15]

Synthesis, Isolation, and Characterization of Sc_2C_2@C_s(6)-C_{82}. Soot containing Sc-EMFs (both the normal sample and the 15% ^{13}C-enriched material) were synthesized with an improved arc-discharge method reported previously.[4e] The Sc_2C_{84} isomer under study is isolated using a four-step HPLC separation (Figure S1, Supporting Information), and its purity was estimated to be higher than 99% with both mass spectrometry and HPLC analysis (Figure S2, Supporting Information). This isomer corresponds to the Sc_2C_{84}(I) reported previously; at that time it was assumed as Sc_2@C_s(10)-C_{84}.[11]

Chemical Functionalization of Sc_2C_2@C_s(6)-C_{82}. In a typical reaction, a flask containing 40 mL of toluene/ODCB (v:v = 9:1) with 5 mg of Sc_2C_2@C_s(6)-C_{82} and an excess amount (ca. 30-fold) of 3-triphenylmethyl-5-oxazolidinone (**1**) was heated under reflux in argon atmosphere.[16] The reaction proceeded smoothly and was monitored with HPLC. After 6 h, the reaction was terminated, and the reaction mixture was concentrated and filtrated for subsequent HPLC separation. Monoadduct **2** was isolated at 70% yield based on consumed Sc_2C_2@C_s(6)-C_{82}.

Black crystals of **2** were obtained by layering a nearly saturated toluene solution at the bottom of hexane in a glass tube (ϕ 7.0 mm) at 253 K. Over a period of two weeks, crystalline rods appeared on the wall of the tube. A piece of crystal with dimension of 0.16 × 0.10 × 0.03 mm was found suitable for the XRD measurement and provided the corresponding structural information of **2**.

RESULTS AND DISCUSSION

Structural Elucidation of Sc_2C_2@C_s(6)-C_{82}. NMR spectrometry is a powerful tool for the structural characterization of fullerenes/EMFs, and the use of ^{13}C-enriched samples has proved effective to enhance the signal-to-noise ratio and to ensure the detection of every possible signal. In particular, previous results showed that the signal of the internal C_2 unit of the carbide cluster is only detectable using ^{13}C-enriched samples.[4f,g] Figure 1 shows the ^{13}C NMR spectrum of the endohedral enriched with 15% carbon-13 (Figure S2a, Supporting Information). It consists of 44 signals in the aromatic region with a pattern of [38 × 2C, 6 × 1C]. This easily leads to one of the three C_s-symmetric C_{82} cages, instead of any of the 24 C_{84} isomers obeying the isolated pentagon rule.[17] The signal of the internal Sc_2C_2 cluster is readily apparent at 244.4 ppm, further confirming the assignment of the C_{82} cage. This value is similar to those observed with Sc_2C_2@C_{2v}-(5)-C_{80} (231.5 ppm), Sc_2C_2@C_{3v}(8)-C_{82} (253.2 ppm), and Sc_2C_2@D_{2d}(23)-C_{84} (249.2 ppm) but is different from that of $[Sc_3C_2$@I_h(7)-$C_{80}]^-$ anion (328.3 ppm).[4f,g] These imply that the electronic structure of the cage strongly influences the chemical environment of the internal cluster. In addition, the C_2 signal is hardly observed on a normal sample (Figure S4, Supporting Information), showing that the shielding effect of the cage current is really strong.[18]

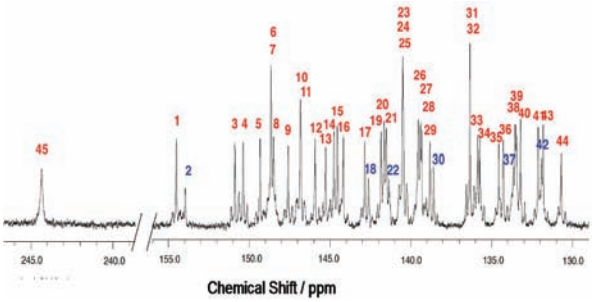

Figure 1. ^{13}C NMR spectrum of 15% ^{13}C-enriched $Sc_2C_2@C_s(6)$-C_{82} measured at 298 K in CS_2. Numbers in red denote peaks with double intensity, whereas single-intensity peaks are marked in blue. The ^{13}C-nuclei signal of the internal Sc_2C_2 unit is readily visible at 244.4 ppm (no. 45).

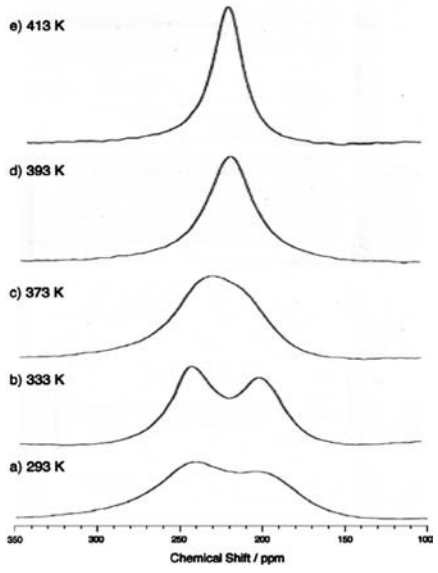

Figure 2. Variable temperature ^{45}Sc NMR spectra of $Sc_2C_2@C_s(6)$-C_{82} measured in ODCB-d_4.

Because three C_s-C_{82} isomers fulfill the ^{13}C NMR pattern, theoretical calculations were relied upon to help with the structure assignment. According to the calculations of Poblet and co-workers,[19] the $C_s(6)$-C_{82} isomer is by no means the most stable one among the three C_s-symmetric C_{82} cages when considering the stability of their tetra-anions. Thus, it is reasonably assigned that Sc_2C_{84}(I) corresponds to $Sc_2C_2@C_s(6)$-C_{82}, not $Sc_2@C_{84}$. This assignment is further confirmed by the X-ray results of its pyrrolidino derivative reported herein.

The temperature-dependent dynamic motion of the internal cluster is a new feature of carbide cluster EMFs. In a previous work on $Sc_2C_2@C_{2v}(5)$-C_{80}, we observed that the internal carbide cluster is highly temperature-sensitive.[4g] A similar phenomenon is also observed in current study of $Sc_2C_2@C_s(6)$-C_{82}, as clearly revealed by ^{45}Sc spectroscopy. The spectra are portrayed in Figure 2: At a temperature under 373 K, two broad peaks are apparent, indicating two nonequivalent Sc atoms within the cage, while the two peaks coalesce into a higher one at temperatures higher than 373 K, featuring a rotating cluster. The inversion barrier can be estimated using the equation: $\Delta G^* = RT_c[22.96 + \ln(T_c/\delta\nu)]$ (cal/mol), where T_c is the coalescence temperature in K and $\delta\nu$ the chemical shift difference in Hz. Employing T_c = 373 K and $\delta\nu$ = 7650 Hz, the energy barrier is calculated as 14.8 kcal/mol. Variable temperature ^{13}C NMR results also confirmed the temperature-dependent motion of the cluster relative to the carbon cage (Figures S5 and S6, Supporting Information).

Scheme 1. Reaction of $Sc_2C_2@C_s(6)$-C_{82} with 1

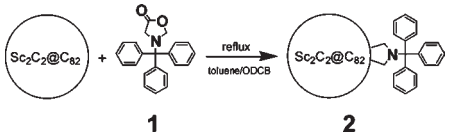

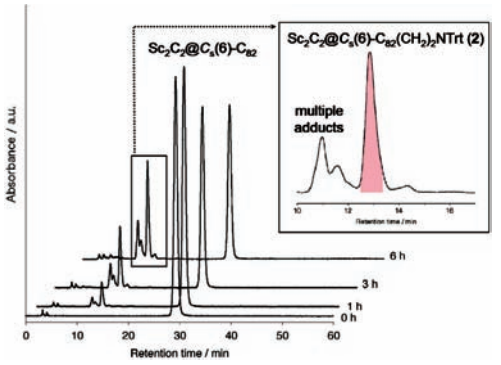

Figure 3. HPLC profiles of the reaction mixture containing $Sc_2C_2@C_s(6)$-C_{82} and **1**. The inset presents an enlarged graph of the adduct peaks.

Chemical Functionalization of $Sc_2C_2@C_s(6)$-C_{82}. The chemical property of $Sc_2C_2@C_s(6)$-C_{82} was investigated by performing the reaction with 3-triphenylmethyl-5-oxazolidinone (**1**). Elevated temperature is necessary for the decarboxylation of **1**, and the resulting 1,3-dipole reacted in situ with the endohedral, forming pyrrolidino-ring fused derivatives (Scheme 1).

The reaction was recorded with HPLC. The profiles of the reaction mixture probed at different reaction times are shown in Figure 3. Before heating, only the peak of starting $Sc_2C_2@C_s(6)$-C_{82} was detected (29.6 min). New peaks appeared between 10 and 14 min after refluxing for 1 h. MALDI-TOF mass spectrometric studies disclosed that the major peak at 12.9 min corresponds to a monoadduct isomer (**2**) and others contain multiple adducts (inset in Figure 3). The reaction was terminated after 6 h, and the monoadduct **2** was isolated at 70% yield based on consumed $Sc_2C_2@C_s(6)$-C_{82}.

The MALDI TOF mass spectrum of **2** is shown in Figure 4. The strongest peak at m/z 1383 clearly confirms the formation of the monoadduct, namely, $Sc_2C_2@C_s(6)$-$C_{82}(CH_2)_2$NTrt (Trt = triphenylmethyl), and the observed isotopic distribution of the ion peak agrees perfectly with the calculated one (insets in Figure 4). The peak at m/z 1098 corresponding to $Sc_2C_2@C_s(6)$-C_{82} is generated via the complete loss of the addend under laser irradiation, and the small peak at m/z 1140 results from the loss of the triphenylmethyl group from **2**.

Since $Sc_2C_2@C_s(6)$-C_{82} has relatively low cage symmetry which consists of 44 different kinds of nonequivalent cage carbons, the regioselective formation of **2** was fairly surprising to us. First of all, we are particularly curious of the molecule structure of **2** which is the basis of any further experimental/theoretical considerations.

dx.doi.org/10.1021/ja208841w |J. Am. Chem. Soc. 2011, 133, 19553–19558

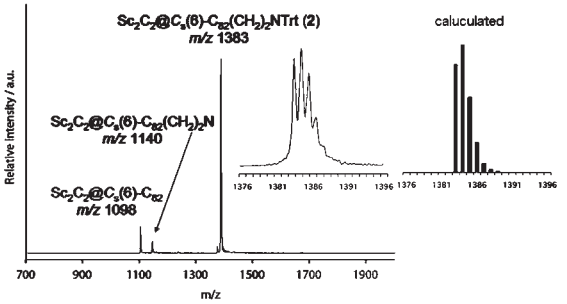

Figure 4. MALDI TOF mass spectrum of **2** in a negative-ion reflection mode. The insets show the observed and calculated isotopic distributions of **2**.

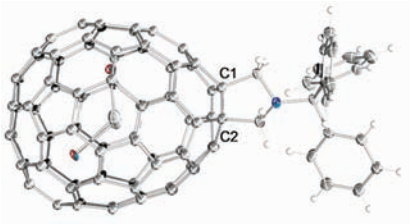

Figure 5. Oak Ridge thermal ellipsoid plot drawing of the major enantiomer of **2** showing thermal ellipsoids at the 50% probability level. Solvent molecules are omitted for clarity.

Crystallization was performed using an interfacial diffusion method, and fortunately, single crystals of **2** were obtained, and its molecular structure was firmly established by single-crystal XRD measurements.

The crystal unit contains a whole molecule of **2**; the unit cavities are filled with a toluene and 1.5 hexane. Disorder exists for the cage, the carbons of the pyrrolidino ring, the internal cluster, and one hexane, while the triphenylmethyl group, the N atom on the pyrrolidine ring, and the toluene are nicely ordered. Four cage orientations with occupancy values of 0.35, 0.30, 0.20, and 0.15, respectively, are distinguished from the X-ray data along with four cluster conformations having the same occupancies. Their matching occupancy values make it easy to pair each cluster conformation with one of the cage orientations. Graphs of the four enantiomers with paired clusters are portrayed in Figure S8, Supporting Information. Because of the severe disorder and the similar occupancy values of the four pairs of structures, enormous structural restrains are applied to regulate the cages not only for the two minor cage orientations but also for the two major ones, which resulted in a low ratio of data-to-parameter. In addition, one of the flexible hexane molecules (solvent) is also disordered, giving highly asymmetric ellipsoids (large Ueq_{max}/Ueq_{min} ratio). Nevertheless, the final structures are chemically reasonable and crystallographically acceptable, especially for such a severely disordered system. Similar phenomena have also been encountered in the refinement processes of other EMFs.[5−7]

Figure 5 shows the major enantiomer of **2** with occupancy of 0.35. It is unambiguous that the EMF takes the $C_s(6)$-C_{82} cage. The triphenylmethyl addend adds to a [6,6]-bond junction abutted by two pentagons, which is very close and nearly parallel to the mirror plane of the C_s-symmetric cage. The C1−C2 bond length is 1.565 Å, confirming a closed cage structure.

The internal Sc_2C_2 cluster is positioned in such a way that neither of the two Sc atoms is close to the addition position. This

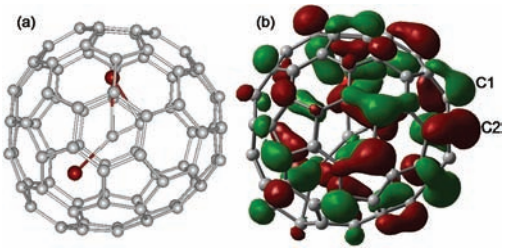

Figure 6. (a) Optimized structure and (b) LUMO orbital of $Sc_2C_2@C_s$-(6)-C_{82}. Both graphs show the same cage orientation as that in Figure 5 for comparison.

differs apparently from the previous observations of the cluster orientation in the corresponding pyrrolidino adducts of other EMFs. For example, the linear La_2 cluster in [6,6]-pyrolidino-$La_2@I_h(7)$-C_{80} is fixed slantwise with one La being trapped inside the cavity of the para-carbon of an addition site,[16] whereas the triangular Sc_3N cluster in [6,6]-$Sc_3N@I_h(7)$-$C_{80}(CH_2)_2$NTrt rotates freely though it is fixed in the corresponding [5,6]-adduct.[20] But in either case, there is at least a metal approaching closely to the para-position of the addition sites. In this regard, the orientation of the carbide cluster in **2** is unique, and this probably originates from the cage symmetry and the rigid shape of the cluster as well.

The bent Sc_2C_2 cluster is like a butterfly. The dihedral angle between the two ScC_2 portions is about 120°, confirming a strong torsion within the cluster. In contrast, a previous crystallographic study of a carbide cluster EMF, i.e., $Gd_2C_2@D_3(85)$-C_{92} showed that the Gd_2C_2 cluster is nearly planar inside the big cage.[21] The C−C bond length (1.213 Å) of the internal cluster Sc_2C_2 in $Sc_2C_2@C_s(6)$-C_{82} represents a typical carbon−carbon triple bond, while the value of the internal C_2 unit in $Gd_2C_2@D_3$-(85)-C_{92} is extraordinarily short, 1.04 Å.[21] Though the nature of the C−C bonding in carbide cluster EMFs is not clear now, the above data indicate that the cage size may not be an important factor for controlling the C−C distance of the internal carbide cluster. The Sc−C distances of the cluster vary in a narrow range of 2.293−2.349 Å. In contrast, the closest contacts between the Sc atoms and the cage carbons are even shorter 2.179 and 2.199 Å, indicating that the bent cluster prefers a flat conformation as much as possible, thus the metals are balanced between the internal C_2 unit and the cage.

Because the addition takes place at a region relatively far from the cluster, it is assumed that the orientation of the cluster is not changed markedly upon functionalization. This speculation is corroborated by our calculations: Starting from the coordinates derived from the X-ray data of **2** (without the pyrrolidine ring), the cluster orientation relative to the cage remains nearly unchanged during the optimization process. The optimized structure of $Sc_2C_2@C_s(6)$-C_{82} is shown in Figure 6a which is nearly identical to that of the X-ray structure of **2** despite the disappearance of the addend. The cluster is also bent with one Sc atom residing under a hexagonal ring and another pointing to a [5,6,6]-junction. The calculated bond lengths are very close to those obtained from the X-ray data of **2**, showing that the chemical transformation of the cage has little effect on the location of the internal carbide cluster.

It has been widely accepted that 1,3-dipolar cycloaddition of azomethine ylides to alkenes (or alkynes) complies with Woodward−Hoffmann rules, thus the addition pattern in **2**

dx.doi.org/10.1021/ja208841w |*J. Am. Chem. Soc.* 2011, 133, 19553–19558

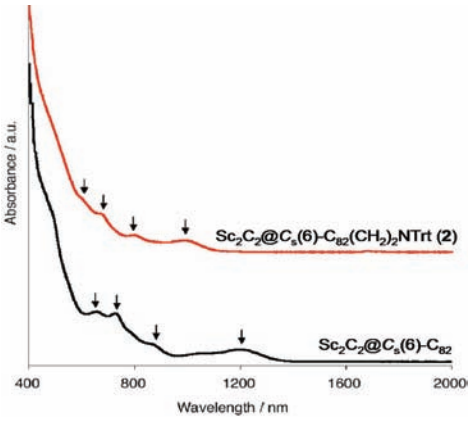

Figure 7. UV−vis NIR spectra of $Sc_2C_2@C_s(6)$-C_{82} and **2**. Absorption peaks are indicated by arrows, and the two curves are vertically shifted for ease of comparison.

can be simply explained by frontier molecular orbital theory. Our calculations show that the highest occupied molecular orbital (HOMO) is mainly localized on the cluster and the cage carbons near the internal metals (Figure S9, Supporting Information), while the lowest unoccupied molecular orbital (LUMO) in $Sc_2C_2@C_s(6)$-C_{82} distributes over the cage carbons relatively far from the metals (Figure 6b). In particular, the carbons of addition (C1 and C2) contain large orbital coefficients in the LUMO, and accordingly they are more favorable to undergo the 1,3-dipolar reaction with **1**. It should be mentioned that the situation in EMFs is far more complicated than that in empty fullerenes (especially C_{60}) because the cage symmetry, the metal composition, orientation, and even motion can have distinct influences on the chemical properties of the molecules. In particular, carbide cluster species have not received equal attention to conventional ones and the nitride cluster EMFs. It is assumed that reasons other than molecular orbital may be also responsible for this high regioselectivity but searching for all possible factors is obviously beyond the scope of this single work.

It was recently reported that the Sc_2S and Sc_2O clusters can also be trapped inside the $C_s(6)$-C_{82} cage.[6,7] Considering the similarity of the electronic structure, cluster orientation, and LUMO distribution among carbide/sulfide/oxide cluster EMFs,[7c] it is speculated that $Sc_2S@C_s(6)$-C_{82} and $Sc_2O@C_s(6)$-C_{82} will also undergo the regioselective reaction with **1** in a similar manner.

Chemical modification of $Sc_2C_2@C_s(6)$-C_{82} has significantly altered its electronic properties. The UV−vis NIR spectra of both pristine $Sc_2C_2@C_s(6)$-C_{82} and **2** are distinctly different from each other, as illustrated in Figure 7. While pristine $Sc_2C_2@C_s(6)$-C_{82} shows distinct absorptions at 662, 731, 867, and 1202 nm, the corresponding bands of **2** are obviously blue shifted to 600, 672, 801, and 988 nm, respectively. In addition, the onset of $Sc_2C_2@C_s(6)$-C_{82} is shifted from 1390 nm (~0.89 eV) to 1150 nm (~1.09 eV) for **2** by chemical modification. Because the cluster orientation is not changed upon chemical modification, it may be conclusive that the electronic properties of both pristine $Sc_2C_2@C_s(6)$-C_{82} and **2** are cage-based.

Electrochemical properties of $Sc_2C_2@C_s(6)$-C_{82} are also affected by the chemical modification. As listed in Table 1, the corresponding redox potentials of $Sc_2C_2@C_s(6)$-C_{82} are cathodically shifted by 0.1−0.3 V, except the irreversible $^{ox}E_2$. The electrochemical bandgap of **2** is 1.58 V, slightly larger than that of pristine $Sc_2C_2@C_s(6)$-C_{82} (1.35 V), indicating that the derivative is more stable. This is consistent with previous results in the chemical functionalization of $La_2@C_{80}$ with **1**, proving that the molecular orbital levels of EMFs can be readily tuned by exohedral modification. It is noteworthy that this is the first report on the electrochemical properties of the derivatives of carbide EMFs.

Table 1. Redox Potentials (V vs Fc/Fc^+)[a] of $Sc_2C_2@C_s(6)$-C_{82} and 2

compound	$^{ox}E_2$	$^{ox}E_1$	$^{red}E_1$	$^{red}E_2$
$Sc_2C_2@C_s(6)$-C_{82}	0.64	0.42	−0.93	−1.30
2	0.65[b]	0.33	−1.25	−1.60

[a] Half cell potentials unless otherwise addressed. [b] Irreversible; DPV peak value.

CONCLUSION

In summary, a Sc_2C_{84} isomer which had been assumed as $Sc_2@C_{84}$ previously, was structurally determined to be $Sc_2C_2@C_s(6)$-C_{82}, thereby adding a new member to the family of metal carbide cluster EMFs. It is again observed that the dynamic motion of the internal Sc_2C_2 cluster is highly temperature dependent. Consequently, this feature is expected to be characteristic of carbide EMFs. In addition, we have investigated for the first time the 1,3-dipolar reaction of metal carbide EMFs using **1**. The 1,3-dipole shows high reactivity and high selectivity to this EMF, affording only one dominant monoadduct (**2**). X-ray data of **2** clearly reveal that the pyrrolidino group is linked to a [6,6]-bond junction far from either of the two Sc atoms, which can be reasonably explained by considering the molecular orbital distributions and the bond strains of the endohedral. Furthermore, it was disclosed that the addition of the addend has no marked influence on the orientation of the internal cluster but significantly alters the electronic and electrochemical properties of the endohedral. Our results have shed new light on the structure of unconventional EMFs and will stimulate greater interests in both experimental and theoretical considerations of metal carbide species. Our achievements are also expected to be useful for future works dealing with the utilization of EMFs as electron-acceptor materials in photovoltaics.[22]

ASSOCIATED CONTENT

Supporting Information. Complete citation of refs 9a and 13, HPLC profiles, mass spectra, CV and DPV curves, NMR spectra, summary of ^{13}C NMR chemical shifts of $Sc_2C_2@C_s(6)$-C_{82}, and X-ray data of **2**. This material is available free of charge via the Internet at http://pubs.acs.org.

AUTHOR INFORMATION

Corresponding Author

*E-mail: akasaka@tara.tsukuba.ac.jp; nagase@ims.ac.jp

ACKNOWLEDGMENT

This work is supported in part by a Grant-in-Aid for Scientific Research on Innovative Areas (no. 20108001, "pi-Space"), a Grant-in-Aid for Scientific Research (A) (no. 20245006), The Next Generation Super Computing Project (Nanoscience Project), Nanotechnology Support Project, Grants-in-Aid for Scientific

Research on Priority Area (nos. 20036008 and 20038007), and Specially Promoted Research (no. 22000009) from the Ministry of Education, Culture, Sports, Science, and Technology of Japan, and The Strategic Japanese-Spanish Cooperative Program funded by JST and MICINN.

REFERENCES

(1) Heath, J. R.; Obrien, S. C.; Zhang, Q.; Liu, Y.; Curl, R. F.; Kroto, H. W.; Tittel, F. K.; Smalley, R. E. *J. Am. Chem. Soc.* **1985**, *107*, 7779–7780.

(2) (a) *Endofullerenes: A New Family of Carbon Clusters*; Akasaka, T., Nagase, S., Eds.; Kluwer: Dordrecht, The Netherlands, 2002. (b) *Chemistry of Nanocarbons*; Akasaka, T., Wudl, F., Nagase, S., Eds.; John Wiley & Sons: *Chichester*, 2010, (c) Lu, X.; Akasaka, T.; Nagase, S. *Rare Earth Metals Trapped inside Fullerenes- Endohedral Metallofullerenes, in Rare Earth Coordination Chemistry: Fundamentals and Applications*; Huang, C. H., Ed.; John Wiley & Sons: Singapore, 2010, pp 273−308.

(3) For recent reviews see: (a) Chaur, M. N.; Melin, F.; Ortiz, A. L.; Echegoyen, L. *Angew. Chem., Int. Ed.* **2009**, *48*, 7514–7538. (b) Yamada, M.; Akasaka, T.; Nagase, S. *Acc. Chem. Res.* **2010**, *43*, 92–102. (c) Dunsch, L.; Yang, S. *Small* **2007**, *3*, 1298–1320. (d) Rodríguez-Fortea, A.; Balch, A. L.; Poblet, J. M. *Chem. Soc. Rev.* **2011**, *40*, 3551–3563. (e) Maeda, Y.; Tsuchiya, T.; Lu, X.; Takano, Y.; Akasaka, T.; Nagase, S. *Nanoscale* **2011**, *3*, 2421–2429.

(4) (a) Takata, M.; Nishibori, E.; Sakata, M.; Inakuma, M.; Yamamoto, E.; Shinohara, H. *Phys. Rev. Lett.* **1999**, *83*, 2214–2217. (b) Wang, C. R.; Kai, T.; Tomiyama, T.; Yoshida, T.; Kobayashi, Y.; Nishibori, E.; Takata, M.; Sakata, M.; Shinohara, H. *Angew. Chem., Int. Ed.* **2001**, *40*, 397–399. (c) Iiduka, Y.; Wakahara, T.; Nakahodo, T.; Tsuchiya, T.; Sakuraba, A.; Maeda, Y.; Akasaka, T.; Yoza, K.; Horn, E.; Kato, T.; Liu, M. T. H.; Mizorogi, N.; Kobayashi, K.; Nagase, S. *J. Am. Chem. Soc.* **2005**, *127*, 12500–12501. (d) Iiduka, Y.; Wakahara, T.; Nakajima, K.; Tsuchiya, T.; Nakahodo, T.; Maeda, Y.; Akasaka, T.; Mizorogi, N.; Nagase, S. *Chem. Commun.* **2006**, 2057–2059. (e) Iiduka, Y.; Wakahara, T.; Nakajima, K.; Nakahodo, T.; Tsuchiya, T.; Maeda, Y.; Akasaka, T.; Yoza, K.; Liu, M. T. H.; Mizorogi, N.; Nagase, S. *Angew. Chem., Int. Ed.* **2007**, *46*, 5562–5564. (f) Yamazaki, Y.; Nakajima, K.; Wakahara, T.; Tsuchiya, T.; Ishitsuka, M. O.; Maeda, Y.; Akasaka, T.; Waelchli, M.; Mizorogi, N.; Nagase, S. *Angew. Chem., Int. Ed.* **2008**, *47*, 7905–7908. (g) Kurihara, H.; Lu, X.; Iiduka, Y.; Mizorogi, N.; Slanina, Z.; Tsuchiya, T.; Akasaka, T.; Nagase, S. *J. Am. Chem. Soc.* **2011**, *133*, 2382–2385. (h) Wang, T. S.; Chen, N.; Xiang, J. F.; Li, B.; Wu, J. Y.; Xu, W.; Jiang, L.; Tan, K.; Shu, C. Y.; Lu, X.; Wang, C. R. *J. Am. Chem. Soc.* **2009**, *131*, 16646–16647. (i) Wang, T. S.; Wu, J. Y.; Xu, W.; Xiang, J. F.; Lu, X.; Li, B.; Jiang, L.; Shu, C. Y.; Wang, C. R. *Angew. Chem., Int. Ed.* **2010**, *49*, 1786–1789.

(5) (a) Stevenson, S.; Rice, G.; Glass, T.; Harich, K.; Cromer, F.; Jordan, M. R.; Craft, J.; Hadju, E.; Bible, R.; Olmstead, M. M.; Maitra, K.; Fisher, A. J.; Balch, A. L.; Dorn, H. C. *Nature* **1999**, *401*, 55–57. (b) Olmstead, M. M.; Lee, H. M.; Duchamp, J. C.; Stevenson, S.; Marciu, D.; Dorn, H. C.; Balch, A. L. *Angew. Chem., Int. Ed.* **2003**, *42*, 900–902. (c) Olmstead, M. H.; de Bettencourt-Dias, A.; Duchamp, J. C.; Stevenson, S.; Marciu, D.; Dorn, H. C.; Balch, A. L. *Angew. Chem., Int. Ed.* **2001**, *40*, 1223–1225. (d) Zuo, T. M.; Beavers, C. M.; Duchamp, J. C.; Campbell, A.; Dorn, H. C.; Olmstead, M. M.; Balch, A. L. *J. Am. Chem. Soc.* **2007**, *129*, 2035–2043. (e) Beavers, C. M.; Chaur, M. N.; Olmstead, M. M.; Echegoyen, L.; Balch, A. L. *J. Am. Chem. Soc.* **2009**, *131*, 11519–11524. (f) Mercado, B. Q.; Beavers, C. M.; Olmstead, M. M.; Chaur, M. N.; Walker, K.; Holloway, B. C.; Echegoyen, L.; Balch, A. L. *J. Am. Chem. Soc.* **2008**, *130*, 7854–7855. (g) Stevenson, S.; Phillips, J. P.; Reid, J. E.; Olmstead, M. M.; Rath, S. P.; Balch, A. L. *Chem. Commun.* **2004**, 2814–2815.

(6) (a) Stevenson, S.; Mackey, M. A.; Stuart, M. A.; Phillips, J. P.; Easterling, M. L.; Chancellor, C. J.; Olmstead, M. M.; Balch, A. L. *J. Am. Chem. Soc.* **2008**, *130*, 11844–11845. (b) Mercado, B. Q.; Olmstead, M. M.; Beavers, C. M.; Easterling, M. L.; Stevenson, S.; Mackey, M. A.; Coumbe, C. E.; Phillips, J. D.; Phillips, J. P.; Poblet, J. M.; Balch, A. L. *Chem. Commun.* **2010**, *46*, 279–281.

(7) (a) Dunsch, L.; Yang, S. F.; Zhang, L.; Svitova, A.; Oswald, S.; Popov, A. A. *J. Am. Chem. Soc.* **2010**, *132*, 5413–5421. (b) Chen., N.; Chaur, M. N.; Moore, C.; Pinzon, J. R.; Valencia, R.; Rodriguez-Fortea, A.; Poblet, J. M.; Echegoyen, L. *Chem. Commun.* **2010**, *46*, 4818–4820. (c) Mercado, B. Q.; Chen, N.; Rodriguez-Fortea, A.; Mackey, M. A.; Stevenson, S.; Echegoyen, L.; Poblet, J. M.; Olmstead, M. M.; Balch, A. L. *J. Am. Chem. Soc.* **2011**, *133*, 6752–6760. (d) Wang, T. S.; Feng, L.; Wu, J. Y.; Xu, W.; Xiang, J. F.; Tan, K.; Ma, Y. H.; Zheng, J. P.; Jiang, L.; Lu, X.; Shu, C. Y.; Wang, C. R. *J. Am. Chem. Soc.* **2010**, *132*, 16362–16364.

(8) Lu, X.; Akasaka, T.; Nagase, S. *Chem. Commun.* **2011**, *47*, 5942–5957.

(9) (a) Maeda, Y.; et al. *J. Am. Chem. Soc.* **2004**, *126*, 6858–6859. (b) Lu, X.; Nikawa, H.; Feng, L.; Tsuchiya, T.; Maeda, Y.; Akasaka, T.; Mizorogi, N.; Slanina, Z.; Nagase, S. *J. Am. Chem. Soc.* **2009**, *131*, 12066–12067. (c) Feng, L.; Nakahodo, T.; Wakahara, T.; Tsuchiya, T.; Maeda, Y.; Akasaka, T.; Kato, T.; Horn, E.; Yoza, K.; Mizorogi, N.; Nagase, S. *J. Am. Chem. Soc.* **2005**, *127*, 17136–17137. (d) Lu, X.; Nikawa, H.; Tsuchiya, T.; Akasaka, T.; Toki, M.; Sawa, H.; Mizorogi, N.; Nagase, S. *Angew. Chem., Int. Ed.* **2010**, *49*, 594–597. (e) Maeda, Y.; Sato, S.; Inada, K.; Nikawa, H.; Yamada, M.; Mizorogi, N.; Hasegawa, T.; Tsuchiya, T.; Akasaka, T.; Kato, T.; Slanina, Z.; Nagase, S. *Chem.—Eur. J.* **2010**, *16*, 2193–2197.

(10) Cardona, C. M.; Kitaygorodskiy, A.; Echegoyen, L. *J. Am. Chem. Soc.* **2005**, *127*, 10448–10453.

(11) Inakuma, M.; Yamamoto, E.; Kai, T.; Wang, C. R.; Tomiyama, T.; Shinohara, H.; Dennis, T. J. S.; Hulman, M.; Krause, M.; Kuzmany, H. *J. Phys. Chem. B* **2000**, *104*, 5072–5077.

(12) Sheldrick, G. M. *Acta Crystallogr.* **2008**, *A64*, 112–122.

(13) Frisch, M. J.; et al. *GAUSSIAN 03*, revision C. 01, Gaussian Inc.: Wallingford, CT, 2004.

(14) (a) Binkley, J. S.; Pople, J. A.; Hehre, W. J. *J. Am. Chem. Soc.* **1980**, *102*, 939–947. (b) Hay, P. J.; Wadt, W. R. *J. Chem. Phys.* **1985**, *82*, 299–310. (c) Hariharan, P. C.; Pople, J. A. *Theor. Chim. Acta* **1973**, *28*, 213–222. (d) Cao, X. Y.; Dolg, M. *J. Mol. Struct. (Theochem)* **2002**, *581*, 139–147.

(15) (a) Becke, A. D. *Phys. Rev. A* **1988**, *38*, 3098–3100. (b) Becke, A. D. *J. Chem. Phys.* **1993**, *98*, 5648–5652. (c) Lee, C.; Yang, W.; Parr, R. G. *Phys. Rev. B* **1988**, *37*, 785–789.

(16) Yamada, M.; Wakahara, T.; Nakahodo, T.; Tsuchiya, T.; Maeda, Y.; Akasaka, T.; Yoza, K.; Horn, E.; Mizorogi, N.; Nagase, S. *J. Am. Chem. Soc.* **2006**, *128*, 1402–1403.

(17) *An Atlas of Fullerenes*; Fowler, P. W. Manolopoulos, D. E., Eds.; Clarendon Press: Oxford, 1995.

(18) (a) Ruttimann, M.; Haldimann, R. F.; Isaacs, L.; Diederich, F.; Khong, A.; Jimenez-Vazquez, H.; Cross, R. J.; Saunders, M. *Chem.—Eur. J.* **1997**, *3*, 1071–1076. (b) Johansson, M. P.; Juselius, J.; Sundhilm, D. *Angew. Chem., Int. Ed.* **2005**, *44*, 1843–1846.

(19) Valencia, R.; Rodriguez-Fortea, A.; Poblet, J. M. *J. Phys. Chem. A* **2008**, *112*, 4550–4555.

(20) Cai, T.; Slebodnick, C.; Xu, L.; Harich, K.; Glass, T. E.; Chancellor, C.; Fettinger, J. C.; Olmstead, M. M.; Balch, A. L.; Gibson, H. W.; Dorn, H. C. *J. Am. Chem. Soc.* **2006**, *128*, 6486–6492.

(21) Yang, H.; Lu, C.; Liu, Z.; Jin, H.; Che, Y.; Olmstead, M. M.; Balch, A. L. *J. Am. Chem. Soc.* **2008**, *130*, 17296–17300.

(22) (a) Takano, Y.; Herranz, M. A.; Martin, N.; Radhakrishnan, S. G.; Guldi, D. M.; Tsuchiya, T.; Nagase, S.; Akasaka, T. *J. Am. Chem. Soc.* **2010**, *132*, 8048–8055. (b) Pinzon, J. R.; Gasca, D. C.; Sankaranarayanan, S. G.; Bottari, G.; Torres, T.; Guldi, D. M.; Echegoyen, L. *J. Am. Chem. Soc.* **2009**, *131*, 7727–7734. (c) Guldi, D. M.; Feng, L.; Radhakrishnan, S. G.; Nikawa, H.; Yamada, M.; Mizorogi, N.; Tsuchiya, T.; Akasaka, T.; Nagase, S.; Herranz, M. A.; Martin, N. *J. Am. Chem. Soc.* **2010**, *132*, 9078–9086. (d) Feng, L.; Radhakrishnan, S. G.; Mizorogi, N.; Slanina, Z.; Nikawa, H.; Tsuchiya, T.; Akasaka, T.; Nagase, S.; Martin, N.; Guldi, D. M. *J. Am. Chem. Soc.* **2011**, *133*, 7608–7618.